Accepted Manuscript

Curing rate effects on the toughness of epoxy polymers

D. Incerti, T. Wang, D. Carolan, A. Fergusson

Please cite this article as: Incerti D, Wang T, Carolan D, Fergusson A, Curing rate effects on the toughness of epoxy polymers, *Polymer* (2018), doi: https://doi.org/10.1016/j.polymer.2018.11.008.

This is a PDF file of an unedited manuscript that has been accepted for publication. As a service to our customers we are providing this early version of the manuscript. The manuscript will undergo copyediting, typesetting, and review of the resulting proof before it is published in its final form. Please note that during the production process errors may be discovered which could affect the content, and all legal disclaimers that apply to the journal pertain.
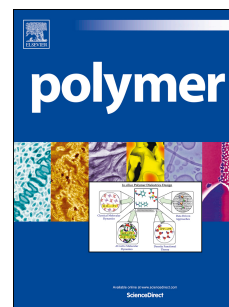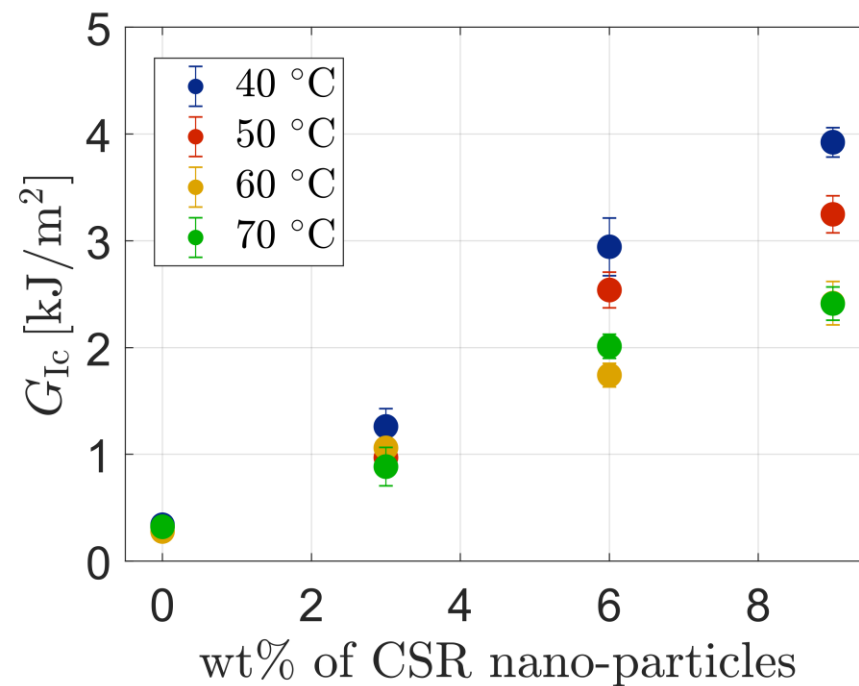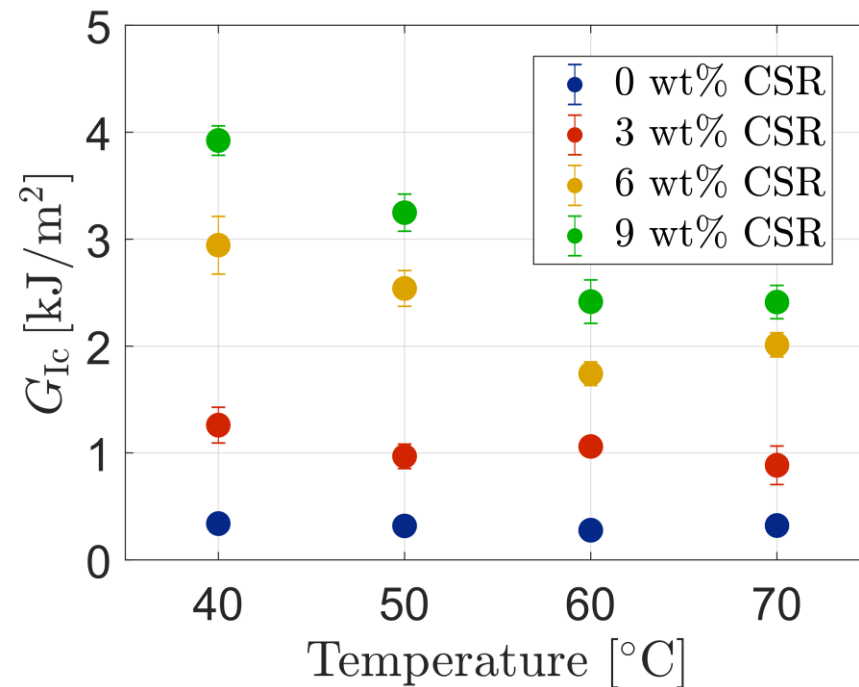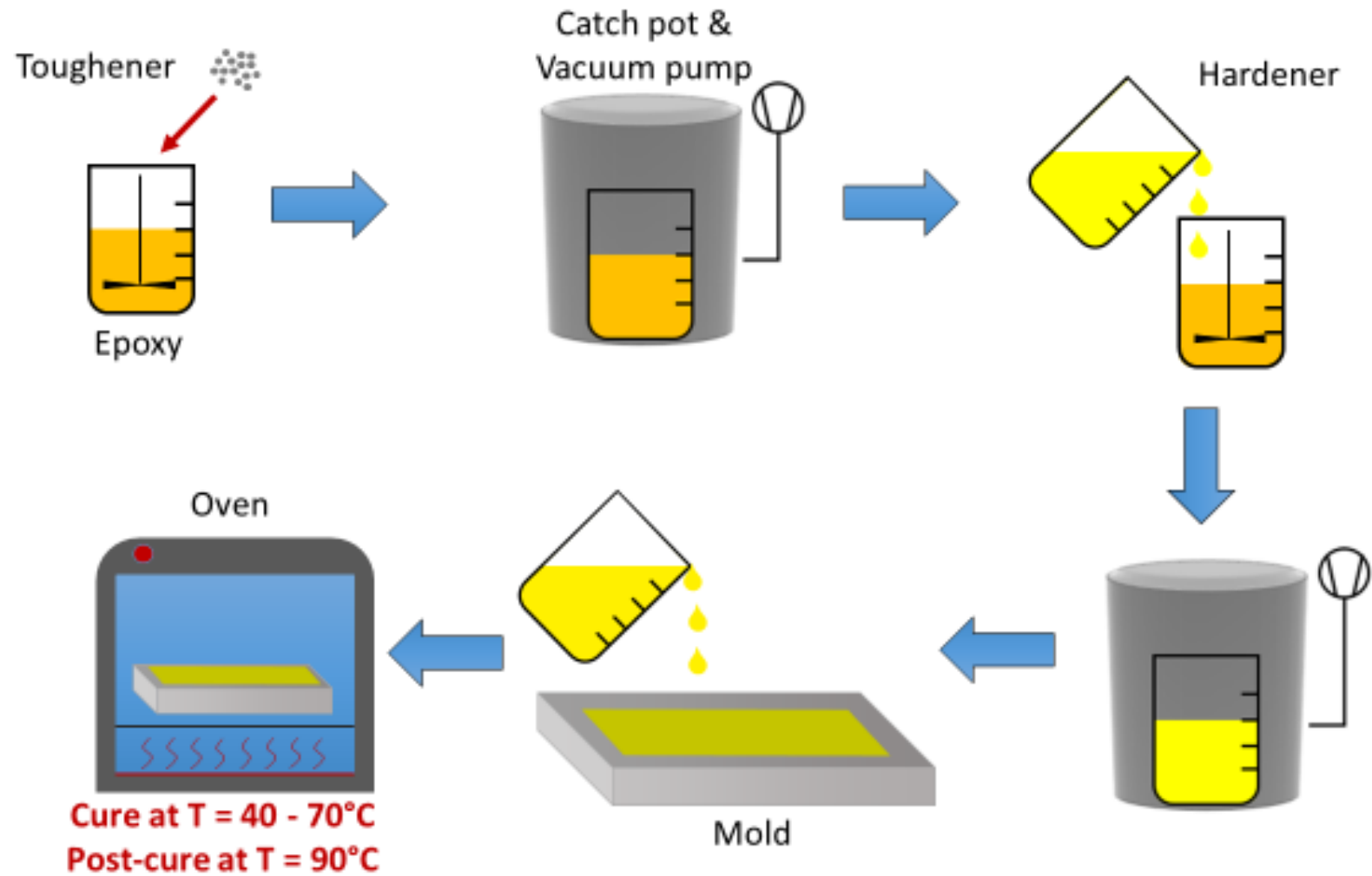
Curing rate effects on the toughness of epoxy polymers

D. Incerti[a,b], T. Wang[a], D. Carolan[a,c], A. Fergusson[a,c]

[a]*FAC Technology, 53 Lydden Grove, London, SW18 4LW, United Kingdom*
[b]*Department of Aeronautics, Imperial College London, Exhibition Road, London, SW7 2AZ, United Kingdom*
[c]*Department of Mechanical Engineering, Imperial College London, Exhibition Road, London, SW7 2AZ, United Kingdom*

Abstract

In the current work, the fracture properties of epoxy polymers containing polysiloxane core shell rubber (CSR) nano-particles were studied. The effect of different cure rates and curing temperatures on the epoxy resin was also investigated. Single edge notched bend tests were performed to evaluate the fracture energy of the polymers. The fracture energy of the unmodified epoxy polymer increased significantly from $339\,\mathrm{J/m^2}$ to $3,922\,\mathrm{J/m^2}$ due to the addition of 9 wt% of CSR nano-particles. Similarly, the fracture toughness for the unmodified polymer increased from $1.27\,\mathrm{MPa\,m^{1/2}}$ to $3.42\,\mathrm{MPa\,m^{1/2}}$ for an epoxy polymer containing 9 wt% of CSR nano-particles. Faster rates of curing, which can be achieved at higher cure temperatures are found to be detrimental to the toughness of the modified epoxy polymers.

1. Introduction

Epoxy polymers are used extensively in aerospace, automotive and electronics applications in the form of adhesives, surface coatings and advanced composite materials. The widespread use of epoxy materials in engineering applications is due to their outstanding mechanical properties such as high stiffness and high strength combined with low density which results in high performance lightweight structures.

The high degree of chemical cross-linking provides outstanding thermal and chemical resistance in epoxy polymers. However, the cross-linked network struc-

ture is also responsible for the brittle behavior associated with unmodified epoxy polymers. The addition of modifiers to toughen the polymer can alleviate this undesired brittleness. Soft rubber particles have been the most successful method to enhance the toughness of epoxy polymers [1, 2, 3, 4].

Two methods can be used to nano-modify the epoxy polymers with rubbers. The first one is based on reactive oligomers [5, 6, 7, 8, 9]. Reactive liquid rubbers form an adduct with the epoxy resin. During the curing process the rubber spearates to form a distinct second phase of small rubber particles. In the second method, the mechanical properties of epoxies are improved by the addition in the resin of pre-formed elastomeric particles such as core-shell rubber (CSR) [10, 11, 12, 13, 14, 15]. These particles consist of a rubber core surrounded by a thin functionalized glassy shell which inhibits agglomeration of the particles. The advantages offered by using preformed rubber particles rather than particles formed via reaction induced phase separation is a precise knowledge of the particle size distribution. Possible disadvantages are that the preformed particles can be filtered out in resin infusion processes of closely packed systems, although Carolan et al. [16] have recently demonstrated successful infusion of a biaxial textile carbon fiber fabric with an epoxy polymer modified with up to 16 wt% of CSR particles. The principal toughening mechanisms associated with polymers modified with rubber micro- or nano-particles have been identified as matrix shield yielding, particle cavitation and matrix plastic void growth [17, 18, 19, 20].

The manufacturing processes involved in the formation of toughened epoxy polymers can have a great impact on the material properties and thermal processing can alter the effectiveness of the tougheners. The performance of the final product greatly depends on several phenomena which take place during the curing process: thermal expansion, chemical shrinkage and material degradation or relaxation [21].

From a commercial point of view, minimizing the cure time by increasing the cure temperature and hence the cure rates of the epoxy systems will lead to a reduction in cost. However, when the cure cycle is accelerated to reduce man-

2

ufacturing time and expense, the possibility of a runaway exotherm is increased. As the cross-linking reaction proceeds, heat is released. This promotes further cross-linking of the resin and hardening products. This then results in a rise in temperature of the cured system. If the temperature rise within the curing epoxy polymer is too great, then degradation and breakdown of the epoxy resin will occur. To date, studies on the curing kinetics of epoxy polymers have been focused on avoiding uncontrolled exotherms which could lead to the cracking of the polymer [22, 23] The addition of ceramic [24] or silica nano-particles [25, 26] has been reported recently to reduce the shrinkage of the resin due to cure and reduce the exotherm by increasing the thermal conductivity of the epoxy polymer.

Very little attention, however has been devoted to the effect of fast cure rates on toughened epoxy polymers besides the work conducted by Keller et al. [27] which simultaneously addresses the role of toughness and fast cure cycle for epoxy matrices. They demonstrate the potential to achieve effective toughening of fast-cure epoxy systems with CSR particles. In the current work, nano-modified epoxy systems containing different weight percentages of CSR particles were analyzed. The cure temperature and hence the cure rate was varied systematically to understand more precisely the relationship between toughness and the rate of cure of the epoxy polymer.

2. Materials and methods

Materials. An amine-based cured diglycidyl ether of bisphenol-A (DGEBA) formed the basis of the different epoxy systems used in the current work. The epoxy resin was a standard DGEBA with an epoxide equivalent weight (EEW) of 185 g/eq. The hardener, developed by FAC Technology, is an amine blend tailored to give a glass transition temperature of circa. 80°C and maximum toughness of the resin.

The resin formulation was altered by replacing 10 wt% of the DGEBA resin with a reactive diluent. The diluent agent was a hexanediol diglycidylether

3

70 (HDDGE) with an EEW of 170 g/eq. The reactive diluent helps the ease of
71 manufacturing by lowering the viscosity of the epoxy resin. The polysiloxane
72 CSR particles were obtained pre-dispersed at 40 wt% in the DGEBA epoxy
73 resin.

74 Formulations containing 3%, 6% and 9% weight percentage of CSR were
75 prepared and cured isothermally at $40°C$, $50°C$, $60°C$ and $70°C$. The stoichio-
76 metric ratios of resin to hardener were modified to account for the presence
77 of the diluent agent and the toughening additives. All formulations were post
78 cured at $90°C$ for 2 hours and cooled to room temperature inside an oven at
79 a low rate of $\approx 1°C/min$ in order to mitigate against the influence of thermal
80 induced residual stresses.

81 *Mechanical properties.* Tensile tests were performed on both the unmodified and
82 nano-modified epoxy systems to obtain the tensile Young's modulus according
83 to ISO-527 [28]. The tests were conducted with dumbbell shaped specimens of
84 type 5A with a gauge length of 30mm, obtained from 3mm thick cast plates. The
85 tests were carried out at a constant cross-head displacement rate of 1 mm/min.
86 The strains were obtained by means of a clip-gauge extensometer. At least five
87 specimens were tested for each formulation in order to assess the repeatability
88 of the results.

89 Uniaxial compression tests were performed to obtain the compressive Young's
90 modulus and the compressive yield stress according to ISO-604 [29]. Polished
91 test samples with dimensions of $16 \times 8 \times 8\,\mathrm{mm}^3$ were loaded in compression be-
92 tween two parallel disks at a constant cross-head displacement rate of 1mm/min.
93 A correction factor was introduced to account for the effects of system compli-
94 ance, loading-pin penetration, and sample compression.

95 Plane strain compressions tests were performed on the unmodified epoxy
96 systems cured at different temperatures following the procedure described by
97 Williams and Ford [30]. Polished test samples with dimensions of $40 \times 40 \times 3\mathrm{mm}^3$
98 were used to obtain the compressive yield stress, σ_{yc}, and failure strain, γ_f.

4

99 *Fracture toughness.* Single-edge notched bending (SENB) tests were performed

100 to obtain the fracture toughness, K_{Ic}, and fracture energy, G_{Ic}, in the opening

101 mode (mode I) according to the ASTM standard [31].

102   Test samples with dimensions of $80 \times 16 \times 8\,\mathrm{mm}^3$ were machined from plates

103 and were notched to a depth of 6 mm. A sharp crack to a depth of $\approx 8\,\mathrm{mm}$ was

104 subsequently introduced by tapping a liquid nitrogen chilled razor blade into the

105 notch. The tests were carried out at a constant cross-head displacement rate of

106 1mm/min under three-point bending. The span used for SENB tests was 64mm.

107 The length of the cracks was measured post-failure using an optical microscope.

108 At least six specimens were tested for each formulation. The fracture toughness

109 was obtained via:

$$K_{\mathrm{Ic}} = \frac{P}{bw^{1/2}}\, f(\frac{a}{w}) \tag{1}$$

110   where P is the failure load, b and w are the thickness and width of the

111 specimen, respectively, and $f(a/w)$ is a fitting function depending on the crack

112 length, a. The fracture energy was computed using the energy method approach

113 via:

$$G_{\mathrm{Ic}} = \frac{U}{bw\phi} \tag{2}$$

114 where U is the energy under the corrected load-displacement curve and ϕ is an

115 energy calibration factor as defined in the ASTM standard [31].

116 *Microscopy.* Fractography studies some characteristic features on the fracture

117 surface of a material that can only be observed using a scanning electron mi-

118 croscopy (SEM). For the purpose of this paper, fractography was used to vali-

119 date the presence of voids and to determine their volume fraction on the fracture

120 surface of SENB samples. Previous studies [16] have shown that if void growth

121 has occurred during fracture, the diameters of the cavitated particles are sig-

122 nificantly bigger than the corresponding diameters measured prior to fracture.

123 To investigate further the fracture mechanisms a field-emission gun scanning-

124 electron microscope (FEGSEM) was used to study the morphology of the SENB

5

125 specimens. Prior to investigation and to reduce build up of electrical charge of

126 the fracture surfaces, the samples were sputter-coated with a 5 nm Au-Pd coat-

127 ing.

128 3. Results and discussion

129 *Tensile properties.* An elastic modulus of 2.57 ± 0.09 GPa was measured for the

130 unmodified epoxy system cured at 40°C. The addition of CSR nano-particles

131 leads to a decrease in the measured elastic modulus. A minimum value of

132 Young's modulus of 2.22 ± 0.19 GPa was measured for the epoxy system con-

133 taining 9 wt% of CSR nano-particles.

134 From Figure 1, it is clear that changing the cure temperature doesn't alter

135 the tensile Young's modulus of the material while the wt% of the toughening

136 additives has a significant effect on the modulus of elasticity. As might be

137 expected, the effect of adding nano-modifiers on the composite elastic modulus

138 was found to be dependent on the relative quantity of the nano-reinforcement

139 added.

140 The experimental results were compared to the predictions obtained from the

141 Halpin-Tsai model [32]. The Halpin-Tsai approach is a semi-empirical model

142 that predicts the composite modulus, E_c, as a function of the epoxy matrix

143 modulus, E_m, and the toughening particles modulus E_p. The tensile composite

144 modulus is obtained via:

$$E_c = \frac{1 + \zeta \, \eta \, v_f}{1 - \eta \, v_f} \, E_m \tag{3}$$

145 where ζ is a shape factor which takes into account the aspect ratio of the par-

146 ticles, v_f, is the volume fraction of the reinforcing particles and the parameter,

147 η, is given by:

$$\eta = \frac{(E_p/E_m) - 1}{(E_p/E_m) + \zeta} \tag{4}$$

148 A shape factor of $\zeta = 2$ was used for the present predictions of the elastic

149 modulus for nano-modified epoxy systems. The aforementioned shape factor

6

150 was suggested by Halpin and Kardos for spherical particles after comparing the

151 theoretical predictions with finite element analysis results [33].

152 Figure 1 shows a very good agreement between the experimentally measured

153 elastic moduli and the semi-empirical predictions obtained with the Halpin-Tsai.

154 *Compressive properties.* The mean values of the uniaxial compressive modulus,

155 E_{uc}, and the uniaxial compressive true yield stress, $\sigma_{y,uc}$ are presented in Table

156 1. For the epoxy systems modified with CSR particles, the compressive modulus

157 and compressive yield stress decrease with the rubber content, a trend which

158 agrees well with the tensile properties. Plots of representative true stress versus

159 true strain curves are given in Figure 2 for the unmodified epoxy resin and

160 for an epoxy system with 9 wt% of CSR nano-particles . It can be seen that

161 following an initial elastic region, the polymer yields and a post yield response

162 varies from sample to sample. Firstly, the yield stress for both unmodified

163 and epoxy polymers containing 9 wt% of toughening additives increase with an

164 increase in cure temperature. No statistically significant change in compressive

165 modulus was noted. Finally, the addition of CSR particles significantly reduces

166 the magnitude of the post yield softening response of the epoxy polymer.

167 The experimental values obtained for compressive yield stress under plane

168 strain conditions, $\sigma_{y,psc}$, and the failure strain, γ_f of the unmodified epoxy

169 polymers cured at different temperatures are presented in Table 2. Under plane

170 strain conditions, no significant difference in yield stress was observed, although

171 a small reduction in the failure strain was noted at high cure temperatures.

172 The non-increase in yield stress, is in contrast to the results reported for unixial

173 compression. This indicates that a change in the pressure sensitivity of the

174 epoxy polymer has occured [6].

175 *Fracture properties.* A maximum fracture toughness, K_{Ic}, of 1.27 ± 0.18 MPa m$^{1/2}$

176 and maximum fracture energy, G_{Ic}, of 339 ± 77 J/m^2 were measured for the un-

177 modified epoxy polymer. Both values were obtained at a cure temperature of

178 $40°$C.

7

179   The addition of CSR nano-particles to the polymer system increased those
180 values significantly to 3.48 ± 0.27 MPa m$^{1/2}$ for K_{Ic} and 3920 ± 140 J/m^2 for
181 G_{Ic}. The fracture toughness increases by almost 200% when the extent of CSR
182 is increased from 0 wt% to 9 wt%, while the fracture energy increases by ap-
183 proximately 1000% when more rubber particles are added to the epoxy resin.

184   From Figure 3, it is evident that the toughness of the material increases
185 proportionally to the content of CSR nano-particles added to the epoxy matrix.

186   The cure rates and cure temperature do not alter the fracture energy and the
187 fracture toughness for epoxy systems containing only a small amount of CSR (
188 0 wt% and 3 wt%). On the contrary from Figure 4, it is clear that when the
189 amount of rubber particles is significant (6 wt% and 9 wt%), the temperature
190 at which the sample is cured reduces the fracture properties of the material
191 significantly.

192   For example, the fracture energy of an epoxy system modified with 9 wt%
193 of CSR cured at 40°C is 3920 ± 140 J/m^2. This value drops to 2411 ± 156 kJ/m^2
194 when the same formulation is cured at 70°C leading to a loss of toughness which
195 is almost 40%. Similarly the fracture toughness for the same epoxy system was
196 measured to be 3.42 ± 0.17 MPa m$^{1/2}$ at 40°C and 3.02 ± 0.18 MPa m$^{1/2}$ at
197 70°C. In this case, the percentage decrease of toughness is approximately 10%.

198   *Curing rate and toughness.* The principal toughening mechanisms associated
199 with CSR nano-modified polymers [17, 18] are (a) localized plastic shear-yielding
200 of the epoxy polymer and (b) plastic void growth of the matrix initiated by
201 cavitation of the toughening particles.

202   Shear-yielding can be defined as a constant volume process that absorbs
203 energy [34]. For epoxy systems modified with CSR, the rubber particles act as
204 stress concentrators where localized shear bands can originate and this facilitates
205 plastic energy dissipation.

206   Additionally, CSR nano-particles cavitate. The process absorbs little energy
207 in itself, but is paramount to relieve the state of hydrostatic stress ahead of the
208 crack tip by creating a void, which subsequently allows plastic deformation of

8

the epoxy polymer around the void to occur. Plastic void growth can absorb a significant amount of energy and can be observed experimentally using a SEM by comparing the initial size of the included particles with the increased size of the void post fracture.

The fracture surface of nano-modified epoxy systems cured at 40°C can be seen in Figure 5. In each of these micrographs, a well-dispersed microstructure of voids can be clearly observed. As expected when a higher content of CSR is added to the epoxy mixture, a greater density of voids is visible on the fracture surface. The radius of these cavitated particles is larger than the corresponding radius of the nano-particles prior to failure. This phenomenon demonstrates that void growth has occurred and this is well established as one of the main toughening mechanisms in rubber modified epoxy systems.

From Figure 6, it can be seen that curing of this epoxy system at a higher temperature, and hence a faster cure rate, leads to some agglomeration of the particles. This is clearly evident in Figures 6 (b) and (c) containing 6 wt% and 9 wt% of CSR particles respectively. In the first case, Figure 6 (b), some voids are still identifiable as coherent structures and retain a spherical shape, while in the latter case, Figure 6 (c) ellipsoidal voids are identified, which bear no relationship to the preformed CSR particles added at the beginning of the manufacturing process. Those arise due to the agglomeration of multiple CSR particles, the voids in Figure 6 (c) are much larger than those in Figures 6 (a) and (b). On the contrary, when 3 wt% of CSR was added to the epoxy mixture, the voids are still reasonably well dispersed and they manifest on the fracture surface as circular.

By further increasing the cure temperature, as it is shown in Figure 7, the clustering and agglomeration of CSR particles phenomenon can also be observed in epoxy systems containing 6 wt% of CSR nano-particles.

An analysis of Figure 8, it is clear that the fracture surface of epoxy systems with a high content of CSR nano-particles is an incoherent structure where rounded and elongated shapes are surrounded by irregular features which are similar to fractals. The preformed CSR particles are no longer clearly distin-

9

240 guishable on the fracture surface.

241 By comparing the different micro-graphs, it is possible to observe that when
242 the rate of cure of the epoxy resin is increased, the dispersion of the CSR parti-
243 cles is affected. In the epoxy polymer with high content of CSR, the toughening
244 additives interact with each-other, coalesce and as a result the voids observed
245 on the fracture surface are not evenly distributed. Hence, the toughening effect
246 of the CSR nano-particles is inhibited since the growth of the voids surrounding
247 these particles is limited by their surrounding space at the micro-structure of
248 the material.

249 Figure 4 clearly highlights this conclusion since for epoxy systems containing
250 6 wt% and 9 wt% of CSR nano-particles, the fracture energy of the material
251 drops significantly as the cure temperature and rate of cure are increased. For
252 epoxy systems containing either no toughening additives or a comparatively
253 small amount (i.e. 3 wt%), the aforementioned trend is not readily apparent in
254 the experimental results since the CSR nano-particles have enough surrounding
255 matrix material to fully grow and form voids.

256 It is important to note that this is a result of the increase in cure rate and
257 not the increase in cure temperature. In the current work, an increased cure
258 temperature has been used as a proxy for increased cure rate. For an anhydride
259 cured system, e.g. that investigated by Carolan et al. [35], the material was
260 cured at 90°C with a post cure at 160°C. Both of these temperatures exceed
261 the maximum cure temperature in the current work, but the rate of cure in the
262 anhydride cure system will be significantly lower than for the amines investigated
263 in the current work, due to the lower reactivity of the anhydride hardening agent.

264 *The Huang-Kinloch model.* After determining the volume fraction of voids ob-
265 served on the fracture surface via SEM and the volume fraction of particles prior
266 to fracture via AFM, it is now possible to implement the Huang and Kinloch
267 model [17, 18].

268 The model is based on a generalized solution which expresses the fracture
269 energy of a modified polymer, G_c, as the sum of the fracture energy of the

10

270 unmodified epoxy system, G_{cu}, plus the contributions from the shear banding

271 and plastic void growth toughening mechanisms such that:

$$G_c = G_{cu} + \psi \tag{5}$$

272 The nano-particles toughening improvement, ψ, can be expressed as:

$$\psi = \Delta G_s + \Delta G_v \tag{6}$$

273 where ΔG_s and ΔG_v refer to shear banding and plastic void growth, respec-

274 tively. The increase in fracture energy associated with shear banding, ΔG_s, is

275 given via:

$$\Delta G_s = 0.5 V_p \sigma_{yc} \gamma_f F'(r_y) \tag{7}$$

276 where V_p is the volume fraction of the particles, σ_{yc} is the plane strain

277 compressive true yield stress of the matrix and γ_f is the true fracture strain

278 of the unmodified epoxy system. Plane strain compression test can be used to

279 determine both σ_{yc} and γ_f.

280 The remaining term, $F'(r_y)$, is a polynomial function which can be expressed

281 as [36]:

$$
\begin{aligned}
F'(r_y) \quad = \quad & r_y \left[\left(\frac{4\pi}{3V_p} \right)^{\frac{1}{3}} \left(1 - \frac{r_p}{r_y} \right)^3 - \left(\frac{8}{5} \right) \left(1 - \frac{r_p}{r_y} \right) \left(\frac{r_p}{r_y} \right)^{\frac{5}{2}} \right. \\
& \left. - \left(\frac{16}{35} \right) \left(\frac{r_p}{r_y} \right)^{\frac{7}{2}} - 2 \left(1 - \frac{r_p}{r_y} \right)^2 + \left(\frac{16}{35} \right) \right]
\end{aligned}
$$

where r_p is the nano-particle radius and r_y is the increased plastic zone size

due to stress concentrations in the epoxy which can be defined as:

$$r_y = K_{vm}^{\;2} \left(1 + \frac{\mu_m}{\sqrt{3}} \right)^2 r_{yu} \tag{8}$$

282 where K_{vm} is the maximum stress concentration according to the von Mises

283 stresses around a particle and μ_m is the pressure sensitivity coefficient of the

284 epoxy (μ_m has been taken as 0.2 for the epoxy systems analyzed in this work).

11

For rubber modifiers the value of K_{vm} was found to vary linearly as a function of the volume fraction of particles, V_p [37].

$$K_{vm} = 3.9337V_p + 2.1126 \tag{9}$$

Lastly, r_{yu}, is the Irwin prediction of the plastic zone radius under plane-strain conditions which can be expressed as:

$$r_{yu} = \frac{1}{6\pi} \frac{EG_c}{(1 - \nu^2)\sigma_{yt}^2} \tag{10}$$

where σ_{yt} is the tensile yield stress of the epoxy. The increase in fracture energy associated with plastic void growth, ΔG_v, is given via:

$$\Delta G_v = \left(1 - \frac{\mu_m^2}{3}\right)(V_v - V_p)\sigma_y r_{yu} K_{vm}^2 \tag{11}$$

where V_v is the volume fraction of voids measured via SEM and the others parameters have all been mentioned previously.

It was shown by Liang and Pearson [38] that the term $(V_v - V_p)$ is given by:

$$(V_v - V_p) = \left(\frac{v_v}{v_v + v_m} - \frac{v_p}{v_p + v_m}\right) \tag{12}$$

where v_v and v_p are the volume of a single void and a single particle, respectively. The last term, v_m, is the volume of the matrix which can be expressed as:

$$v_m = \frac{v_p}{V_p} - v_p \tag{13}$$

Determination of CSR void growth. To implement the Huang-Kinloch model, the radius of the CSR nano-particles and radius of the subsequent void forming during fracture are needed. Those are required to obtain a numerical value for $(V_v - V_p)$.

Using atomic force microscopy (AFM) images, Carolan et al. [35] showed that the size distribution of the CSR nano-particles can be described by a log-normal distribution with a mean particle radius of 0.08 μm.

12

To determine the radius of a single voids two methods can be used. The first one is based on a conventional approach, measuring manually the radii. Using the SEM images of the fracture surface, the radii of a large number of voids are measured on the fracture surface and afterwards, the mean value of these measurements, $\overline{r}$, is taken as the average void size. The second method assumes that the voids can grow until the failure strain of the matrix, γ_f, is reached. In this case, the radius of the void, r_v, is given as a function of the initial particle radius, r_p, and the matrix failure strain, γ_f, according to the following formula:

$$r_v = r_p(1 + \gamma_f) \qquad (14)$$

The second approach is preferable as it is truly predictive, relying only on independent measurements of mechanical and fracture properties and not on any post-mortem measurements of the fracture surface as in the first approach. Table 3 compares the predictive G_{Ic} values obtained following the two different approaches to the experimental results. A number of observations may be made from the results presented in Table 3. It can be seen that the predictive approach, i.e. the γ_f approach, predicts remarkably well the experimentally measured fracture energies for epoxy polymers modified with 6% and 9% and cured at 40°C. This difference is due to a change in the value of the ΔG_v term in the Huang-Kinloch model. The mean value approach, on the other hand, predicts well the measured fracture energy for the epoxy polymer modified with 3% of CSR particles and cured at 40°C, with a significant over prediction made by assuming the void growth relationship in Equation 14. Similarly, a reasonable prediction of the fracture energy is made by the Huang-Kinloch model using the mean value approach for the epoxy polymer modified with 3% CSR particles and cured at 60°C. Finally, for epoxy polymers cured with 3% CSR particles at a temperature of 70°C, both the $\overline{r}$ and the γ_f approach significantly over-predict the experimentally measured fracture energy. Attempts were made to apply the mean-value Huang-Kinloch model to the micro-structures where an incoherent micro-structure was observed on the fracture surface although the interpreta-

13

332 tion of what constitutes a void proved extremely subjective. The predictive
333 γ_f approach was found to over-predict the experimentally measured fracture
334 energy values. However the over-prediction in these cases was not significantly
335 different from those polymers where a reliable prediction using the mean-value
336 approach could be made.

4. Conclusions

338 The mechanical and fracture properties of epoxy polymers modified with
339 poly-siloxane core-shell rubber (CSR) nano-particles were studied. The effect
340 of cure temperature and rate of cure on these properties was also investigated.
341 Several conclusions can be drawn from the current work.

342 The Youngs modulus of the nano-modified epoxy polymers decreased with
343 increasing the weight fraction (wt%) of CSR nano-particles. A good agreement
344 was found between the experimental results and the elastic properties of the
345 nano-modified epoxies predicted using the Halpin-Tsai model.

346 The compressive modulus and compressive yield stress decrease with the
347 rubber content, a trend which agrees well with the tensile properties. This is
348 due to the softness of the rubber in comparison with the epoxy polymer.

349 The addition of CSR nano-particles to the epoxy matrix leads to a signifi-
350 cant toughening of the polymer. For CSR nano-modified epoxies, the speed of
351 cure is the decisive factor which determines the effectiveness of the toughening
352 additives.

353 When fast cure cycles are applied, the weight fraction of CSR nano-particles
354 present in the epoxy system is the principal indicator of the extent to which the
355 increase in toughness of the epoxy polymer is inhibited. The higher the content
356 of CSR particles, the greater the drop in fracture energy observed experimen-
357 tally.

358 On these grounds, when designing the cure cycle of toughened epoxy systems
359 in an industrial or commercial setting, the detrimental effects on the toughness
360 which arise as a result of both high temperature and faster cure cycles should

14

361   be properly accounted for.

362   **5. Acknowledgements**

References

[1] R. Bagheri, B. T. Marouf, R. A. Pearson, *Rubber-Toughened Epoxies: A Critical Review*. Polymer Reviews. 2009;49(3):201-225.

[2] D. Ratna, A. K. Banthia, *Rubber toughened epoxy*. Macromolecular Research. 2004;12(1):11-21.

[3] B. S. Hayes, J. C. Seferis, *Modification of thermosetting resins and composites through preformed polymer particles: A review*. Polymer Composites. 2001;22(4):451-467.

[4] R. S. Drake, A. R. Siebert, *Reactive Butadiene/Acrylonitrile Liquid and Solid Elastomers: A Bibliography for Formulating Epoxy Structural Adhesives*. Adhesive Chemistry. 1984;:643-654.

[5] N. Chikhi, S. Fellahi, M. Bakar, *Modification of epoxy resin using reactive liquid (ATBN) rubber*. European Polymer Journal. 2002;38(2):251-264.

[6] J. N. Sultan, F. J. McGarry, *Effect of rubber particle size on deformation mechanisms in glassy epoxy*. Polymer Engineering and Science. 1973;13(1):29-34.

[7] A. J. Kinloch, S. J. Shaw, D. A. Tod, D. L. Hunston, *Deformation and fracture behaviour of a rubber-toughened epoxy: 1. Microstructure and fracture studies*. Polymer. 1983;24(10):1341-1354.

[8] J. Szymaska, M. Bakar, A. Biakowska, M. Kostrzewa, *Study on the adhesive properties of reactive liquid rubber toughened epoxy-clay hybrid nanocomposites*. Journal of Polymer Engineering. 2018;38(3):231-238.

[9] Y. J. Lim, D. Carolan, A. C. Taylor, *Simultaneously tough and conductive rubber-graphene-epoxy nanocomposites*. Journal of Materials Science. 2016;51:8631-8644.

[10] A. J. Kinloch, *Toughening Epoxy Adhesives to Meet Today's Challenges*. MRS Bulletin. 2003;28(06):445-448.

16

392 [11] D. Quan, A. Ivankovic, *Effect of coreshell rubber (CSR) nano-particles on*
393 *mechanical properties and fracture toughness of an epoxy polymer*. Polymer.
394 2015;66:16-28.

395 [12] R. A. Pearson, A. F. Yee, *Influence of particle size and particle size dis-*
396 *tribution on toughening mechanisms in rubber-modified epoxies*. Journal of
397 Materials Science. 1991;26(14):3828-3844.

398 [13] J. Chen, A. J. Kinloch, S. Sprenger, A. C. Taylor, *The mechanical properties*
399 *and toughening mechanisms of an epoxy polymer modified with polysiloxane-*
400 *based core-shell particles*. Polymer. 2013;54(16):4276-4289.

401 [14] G. Giannakopoulos, K. Masania, A. C. Taylor, *Toughening of epoxy using*
402 *coreshell particles*. Journal of Materials Science. 2010;46(2):327-338.

403 [15] D. Quan, D. Carolan, C. Rouge, N. Murphy, A. Ivankovic, *Carbon nan-*
404 *otube and core-shell rubber nanoparticles modified structural epoxy adhe-*
405 *sives*. Journal of Materials Science, 2017;52:4493-4508.

406 [16] D. Carolan, A. Ivankovic, A. J. Kinloch, S. Sprenger, A. C. Taylor, *Tough-*
407 *ened carbon fibre-reinforced polymer composites with nanoparticle-modified*
408 *epoxy matrices*. Journal of Materials Science. 2016;52(3):1767-1788.

409 [17] Y. Huang, A. J. Kinloch, *Modelling of the toughening mechanisms in*
410 *rubber-modified epoxy polymers: part I: finite element analysis studies*.
411 Journal of Materials Science, 27(10), pp.2753-2762.

412 [18] Y. Huang, A. J. Kinloch, *Modelling of the toughening mechanisms in*
413 *rubber-modified epoxy polymers: part II: a quantitative description of the*
414 *microstructure-fracture property relationship*. Journal of Materials Science,
415 27(10), pp.2763-2769.

416 [19] R. Bagheri, R. A. Pearson, *Role of particle cavitation in rubber-toughened*
417 *epoxies: 1. Microvoid toughening*. Polymer. 1996;37(20):4529-4538.

17

[20] A. F. Yee, R. A. Pearson, *Toughening mechanisms in elastomer-modified epoxies*. Journal of Materials Science. 1986;21(7):2462-2474.

[21] D. Li, X. Li, J. Dai, *Process Modelling of Curing Process-Induced Internal Stress and Deformation of Composite Laminate Structure with Elastic and Viscoelastic Models*. Applied Composite Materials. 2017.

[22] Z. Guo, S. Du, B. Zhang, *Temperature field of thick thermoset composite laminates during cure process*. Composites Science and Technology. 2005; 65(3-4), pp.517-523.

[23] J. Zhang, Y. C. Xu, P. Huang, *Effect of cure cycle on curing process and hardness for epoxy resin*. Express Polymer Letters. 2009; 3(9), pp.534-541.

[24] J. M. Nelson, A. M. Hine, D. P. Goetz, P. Sedgwick, R. H. Lowe, E. Rexeisen, R. E. King, C. Aitken, Q. Pham, *Properties and Applications of Nanosilica-modified Tooling Prepregs*. SAMPE Journal. 2013; 49. 7-17.

[25] S. Sprenger, M. H. Kothmann, V. Altstaedt, *Carbon fiber-reinforced composites using an epoxy resin matrix modified with reactive liquid rubber and silica nanoparticles*. Composites Science and Technology. 2014; 105, pp.86-95.

[26] A. Keller, K. Masania, A. C. Taylor, C. Dransfeld, *Fast-curing epoxy polymers with silica nanoparticles: properties and rheo-kinetic modelling*. Journal of Materials Science. 2015; 51(1), pp.236-251.

[27] A. Keller, H. M. Chong, A. C. Taylor, C. Dransfeld, K. Masania, *Core-shell rubber nanoparticle reinforcement and processing of high toughness fast-curing epoxy composites*. Composites Science & Technology. 2017; 147, pp.78-88.

[28] ISO 527-1 *Plastics - Determination of tensile properties - Part 1: General Principles*. International Standards Organization: Geneva, 1996.

18

[29] ISO 604 *Plastics   Determination of compressive properties.* International Standards Organization: Geneva, 2002.

[30] J. G. Williams, H. Ford, *StressStrain relationships for some unreinforced plastics.* Journal of Mechanical Engineering Science 1959-1982 (vols 1-23). 1964;6(4):405-417.

[31] *Test Methods for Plane-Strain Fracture Toughness and Strain Energy Release Rate of Plastic Materials.*

[32] J. C. Halpin, J. L. Kardos, *The Halpin-Tsai equations: A review.* Polymer Engineering and Science. 1976;16(5):344-352.

[33] J. C. Halpin, N. J. Pagano, *The Laminate Approximation for Randomly Oriented Fibrous Composites.* Journal of Composite Materials. 1969;3(4):720-724.

[34] C. B. Bucknall, I. K. Partridge, M. V. Ward, *Rubber toughening of plastics.* Journal of Materials Science. 1984, 19(6), pp.2064-2072.

[35] D. Carolan, A. Ivankovic, A. J. Kinloch, S. Sprenger, A. C. Taylor, *Toughening of epoxy-based hybrid nanocomposites.* Polymer. 2016;97:179-190.

[36] T. H. Hsieh, A. J. Kinloch, K. Masania, J. Sohn Lee, A. C. Taylor, S. Sprenger, *The toughness of epoxy polymers and fibre composites modified with rubber microparticles and silica nanoparticles.* Journal of Materials Science. 2009;45(5):1193-1210.

[37] H. M. Chong, *Toughening mechanisms of block copolymer and graphene nanoplatelet modified epoxy poylmers.* Imperial College London; 2015.

[38] Y. L. Liang, R. A. Pearson, *Toughening mechanisms in epoxysilica nanocomposites (ESNs).* Polymer. 2009;50(20):4895-4905.

₄₆₈ **6. Figures**
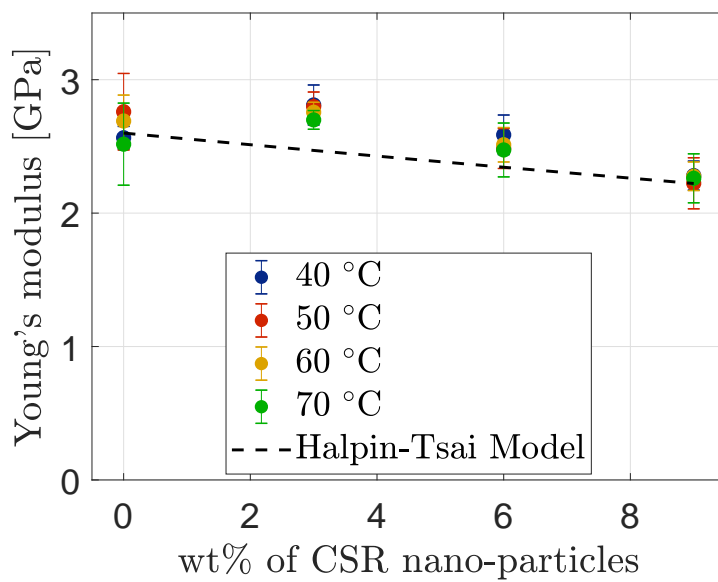
Figure 1: Young's modulus versus weight content of CSR for nano-modified epoxy systems cured at different temperatures.
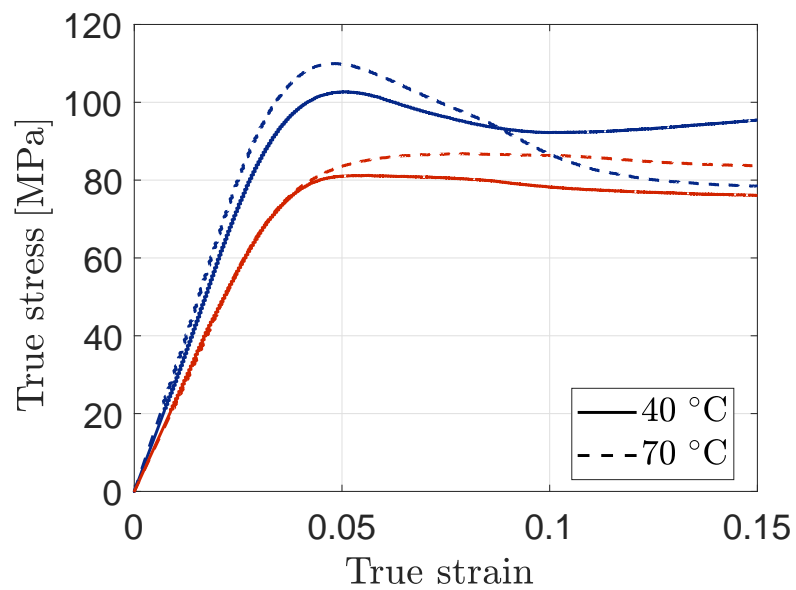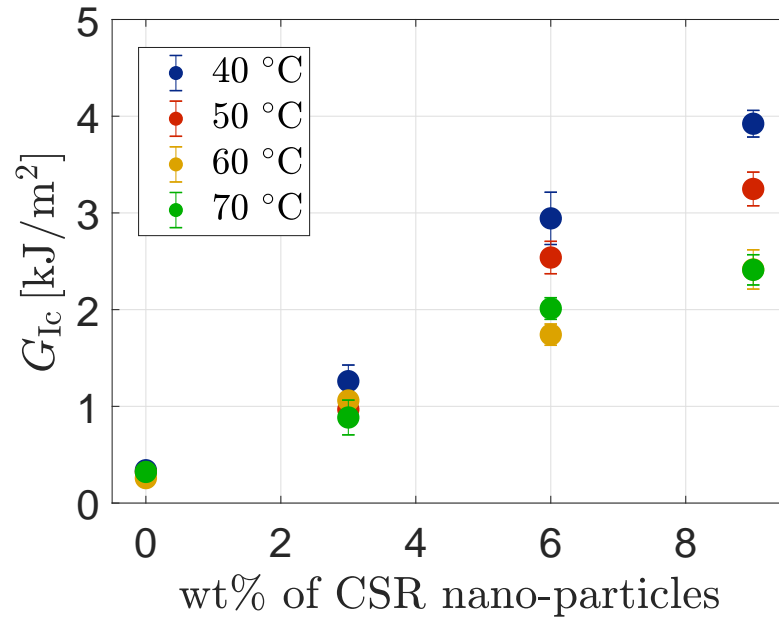
Figure 2: Typical true stress-strain curves at different temperatures for unmodified epoxy system (blue line) and nano-modified epoxy systems containing 9 wt% of CSR (red line).
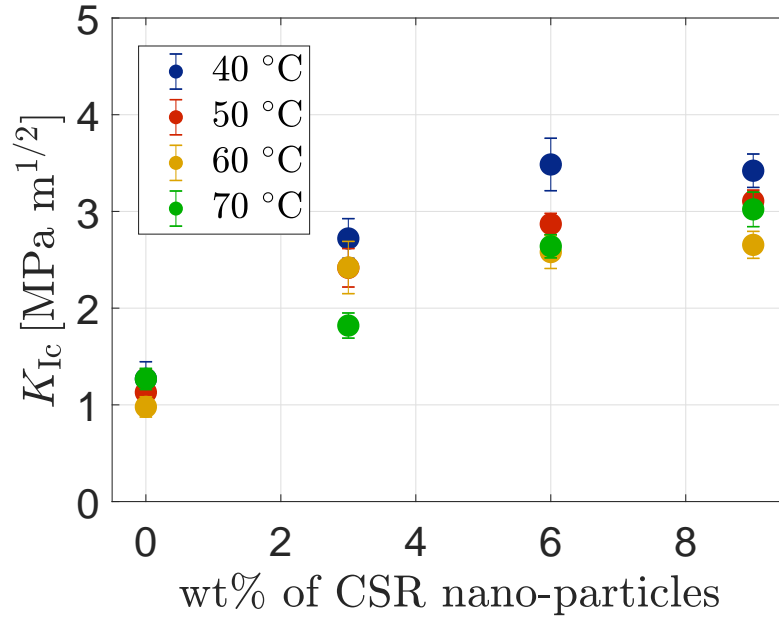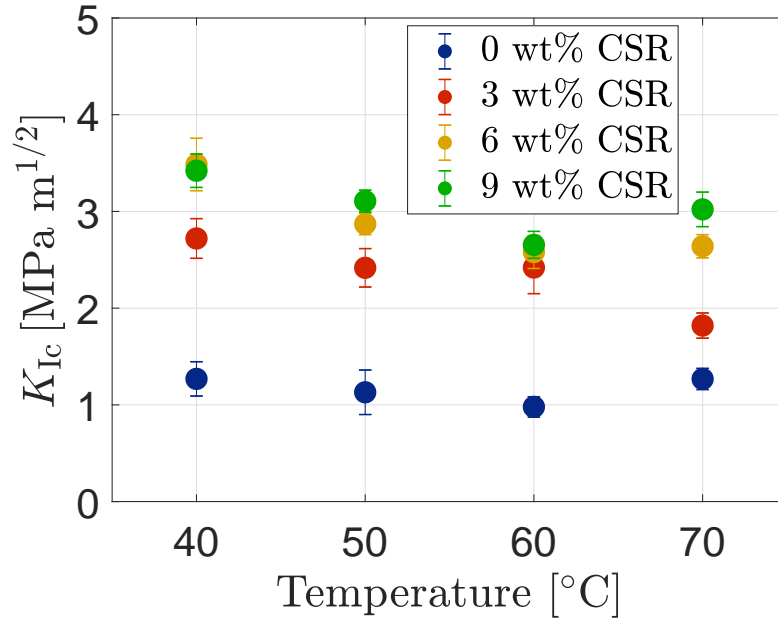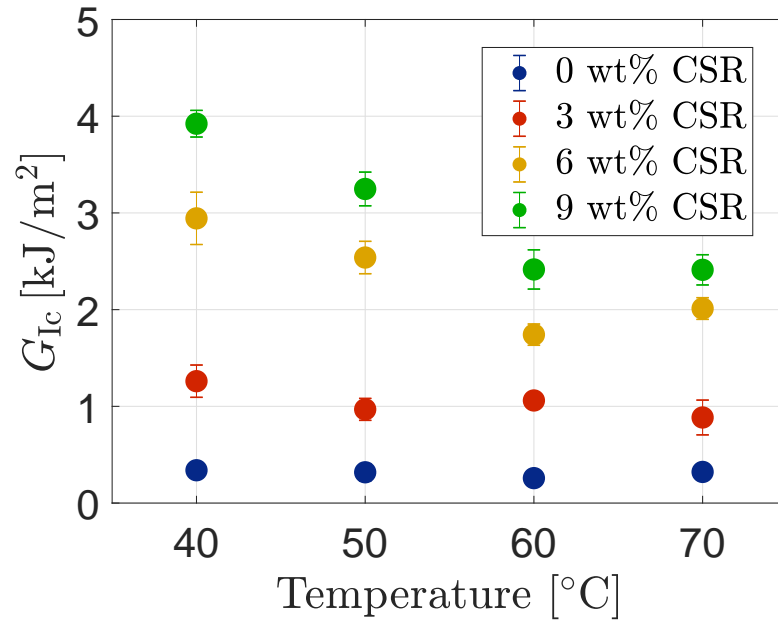
(a)

(b)

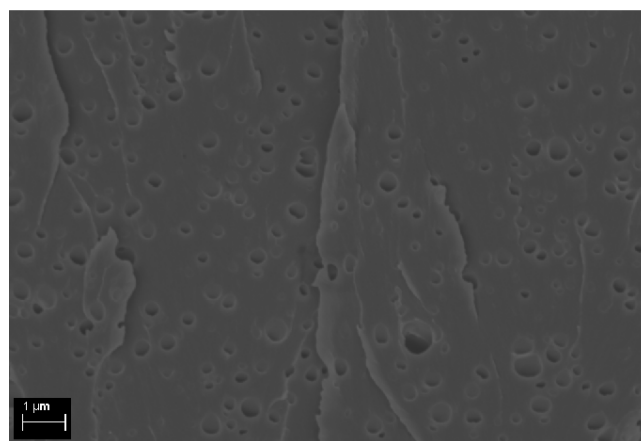Figure 3: Fracture toughness **(a)** and fracture energy **(b)** versus weight percentage of CSR nano-particles.

22

(a)

(b)

Figure 4: Fracture toughness **(a)** and fracture energy **(b)** versus curing temperature for CSR modified epoxy systems.
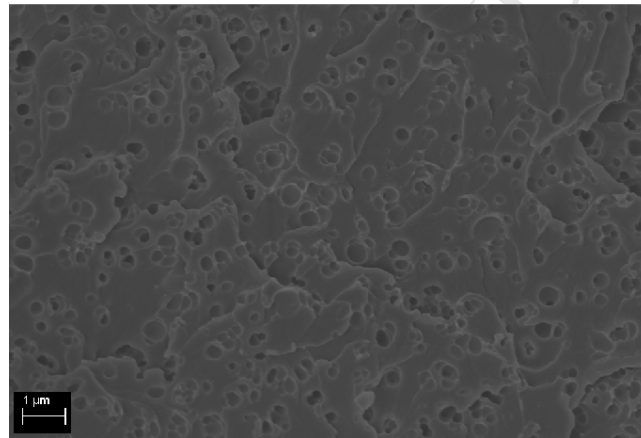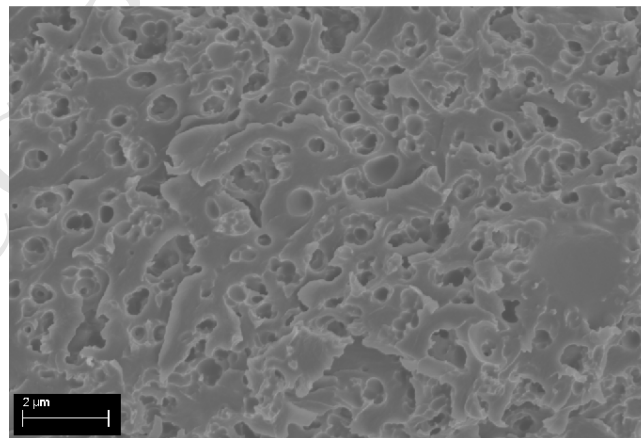
23

(a)
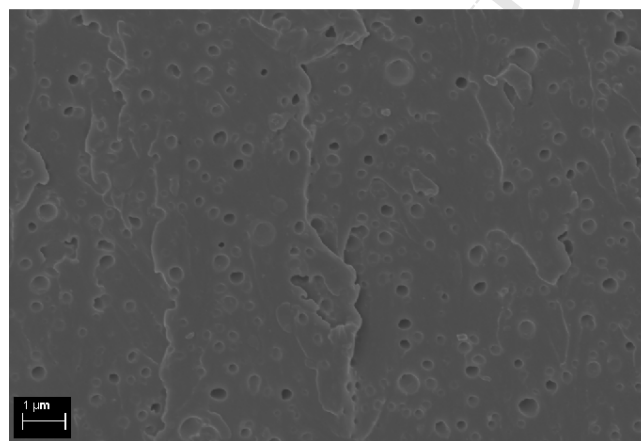
(b)
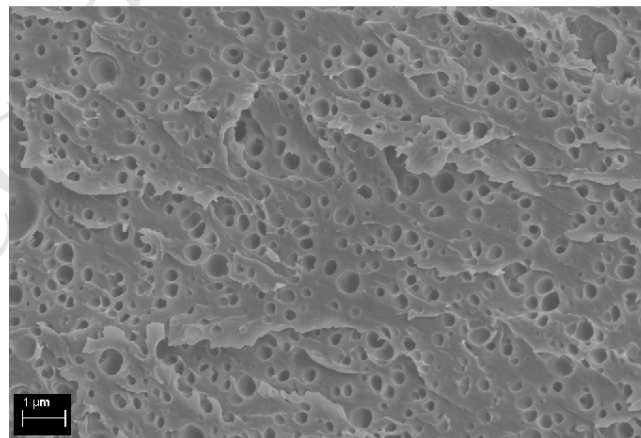
(c)

Figure 5: SEM images of the fracture surface of epoxy systems cured at 40°C containing 3 wt% **(a)**, 6 wt% **(b)** and 9 wt% **(c)** of CSR nano-particles.
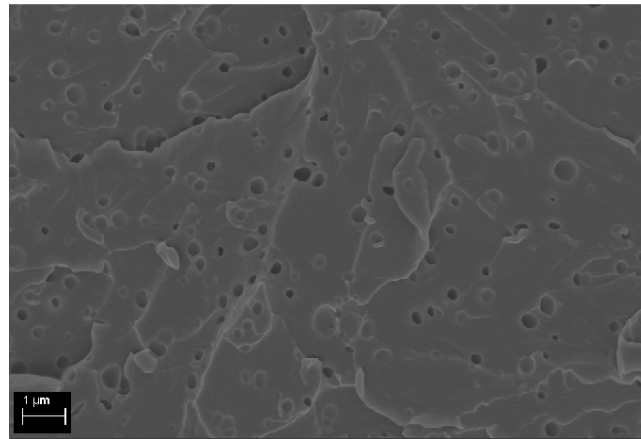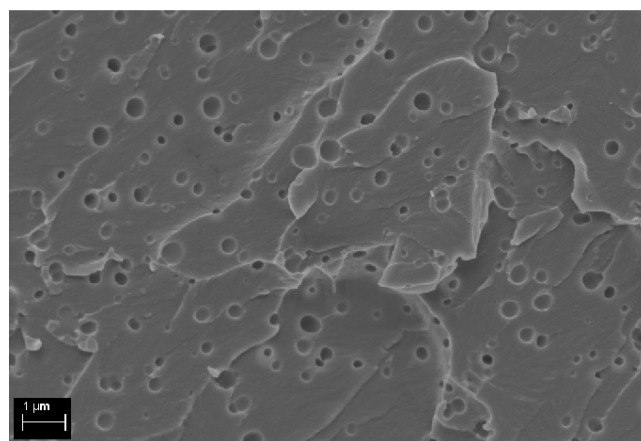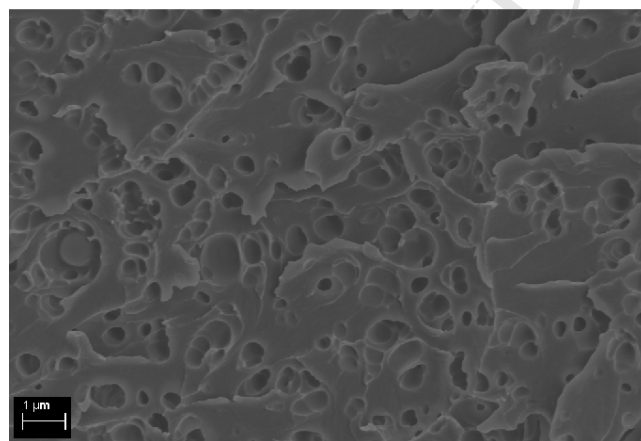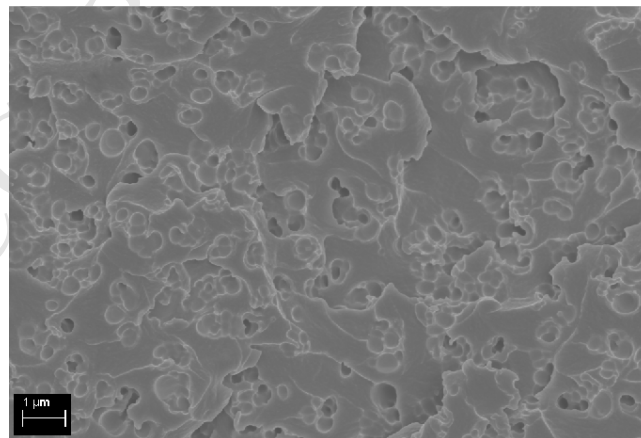
(a)

(b)

(c)

Figure 6: SEM images of the fracture surface of epoxy systems cured at 50°C containing 3 wt% **(a)**, 6 wt% **(b)** and 9 wt% **(c)** of CSR nano-particles.

(a)

(b)

(c)

Figure 7: SEM images of the fracture surface of epoxy systems cured at 60°C containing 3 wt% **(a)**, 6 wt% **(b)** and 9 wt% **(c)** of CSR nano-particles.

(a)

(b)

(c)

Figure 8: SEM images of the fracture surface of epoxy systems cured at 70°C containing 3 wt% **(a)**, 6 wt% **(b)** and 9 wt% **(c)** of CSR nano-particles.

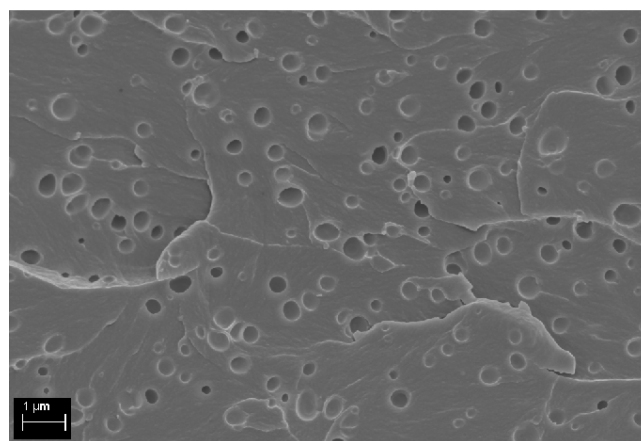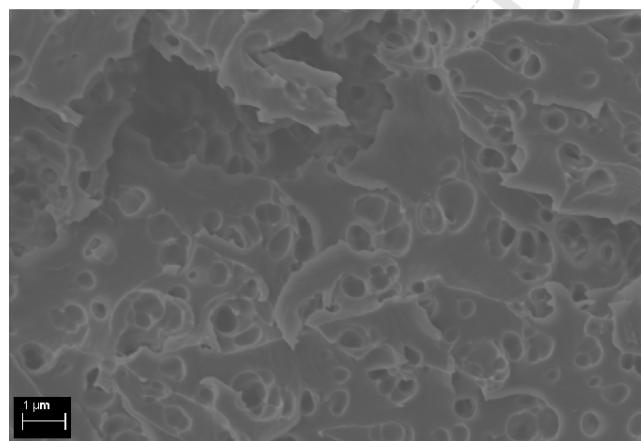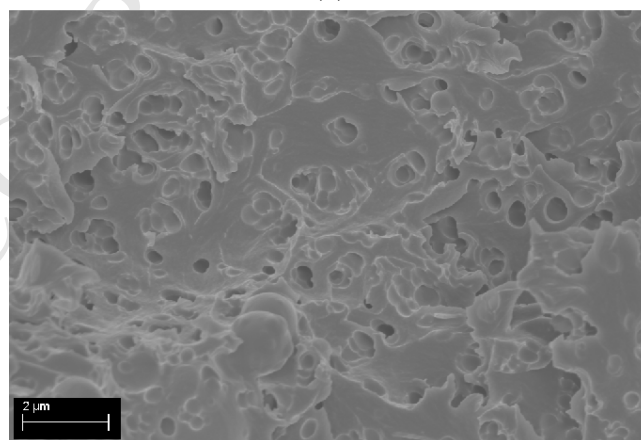469 **7. Tables**

Table 1: Measured unixial compressive properties of polymers.

CSR	40°C		70°C	
(wt%)	σ_{yc}	E_c	$\sigma_{y,uc}$	E_c
	(MPa)	(GPa)	(MPa)	(GPa)
0	104 ± 1	3.1 ± 0.4	111 ± 1	3.0 ± 0.2
9	80 ± 2	2.4 ± 0.1	85 ± 2	2.3 ± 0.1

Table 2: Measured plane strain compressive properties of unmodified polymers.

Temperature	$\sigma_{y,psc}$	γ_f
(°)	(MPa)	(-)
40	99 ± 1	1.07
50	99 ± 1	1.07
60	101 ± 1	0.99
70	100 ± 1	0.97

28

Table 3: Comparison of Huang-Kinloch model toughness predictions with experimental results for CSR nano-modified epoxy systems

CSR (wt%)	Temperature (°)	Experimental results (J/m^2)	H-K model ($\bar{r}$ approach) (J/m^2)	H-K model (γ_f approach) (J/m^2)
3	40	1260 ± 167	1382 (+9.7%)	1940 (+54%)
6	40	2943 ± 270	1894 (−36%)	3125 (+6.2%)
9	40	3922 ± 138	2499 (−36%)	4140 (+5.6%)
3	50	969 ± 114	1314 (+36%)	1940 (+100%)
6	50	2539 ± 167	−	3125 (+23%)
9	50	3248 ± 174	−	4140 (+27%)
3	60	1061 ± 52	1256 (+18%)	1786 (+68%)
6	60	1741 ± 110	−	2892 (+66%)
9	60	2416 ± 203	−	3857 (+60%)
3	70	885 ± 180	1674 (+89%)	1748 (+98%)
6	70	2011 ± 112	−	2834 (+41%)
9	70	2412 ± 156	−	3785 (+57%)

- Epoxy nanocomposites are toughened using core shell rubber particles.

- Measured fracture energy depends on nanocomposite composition and processing history.

- Higher rates of cure lead to a reduction in measured fracture energy.